



Evaluation of Ramucirumab as a combinational cancer therapeutic with 5-Aza- citidine in human Hepatoma (HuH-7) cell line

Hadeel Almasoud^{*}, Saud Alarifi, Saad Alkahtani

Department of Zoology, College of Science, King Saud University, P. O. Box 2455, Riyadh 11451, Saudi Arabia

ARTICLE INFO

Keywords:

Ramucirumab
5-Aza
Apoptosis
Hepatocellular carcinoma
Oxidative stress

ABSTRACT

The purpose of this study is to explore the impact of Ramucirumab alone and combined with 5-Aza on different cellular targets in human hepatocellular carcinoma cell line (HuH-7). Cells were treated with diverse concentrations of Ramucirumab (50, 100, 150 µg/mL) for 24 h. viability, levels of reactive oxygen species (ROS), antioxidant activities, mitochondrial membrane potential (MMP), DNA fragmentation, and expression of apoptotic genes (Caspases 3, 7, 9, p53, Bax, and Bcl-2) were measured. Results showed that HuH-7 cell viability was reduced in dose-dependent way with Ramucirumab therapy. Both Ramucirumab and 5-Aza elevated ROS, but their combination reduced ROS levels, though still higher than controls. Ramucirumab decreased SOD activity; while 5-Aza increased it. Combined therapy potentially increased SOD and CAT activities. Ramucirumab alone was not responsible to influence GSH levels, but 5-Aza and the combination treatments increased GSH levels. All treatments reduced the JC-1 aggregate/monomer ratio, indicating decreased MMP and potential apoptosis induction. High fragmented DNA and condensation of chromatin were recorded suggesting apoptosis. Both agents, either as monotherapy or combined therapy, upregulated Caspases 3, 7, and 9, p53, and Bax expression, with variable effects on Bcl-2. In conclusion, Ramucirumab, particularly when co-administered with 5-Aza, effectively reduces viability of cells and prompts apoptosis in HuH-7 cells through increased oxidative stress, disturbance of MMP, and apoptotic pathways activation. The combination treatment shows potential for enhanced therapeutic efficacy against hepatocellular cancer cells.

1. Introduction

Hepatocellular carcinoma (HCC) remains a significant global health burden, with limited therapeutic choices and dismal prognosis, particularly when disease is advancing (Sung et al., 2021). Despite innovation in treatment methods, encompassing surgical resection, liver transplantation, and systemic therapies, the outcomes for progressive HCC cases remain unsatisfactory. The 5-year survival for advanced HCC stands at approximately 12 %, highlighting the pressing requirement for additional research and enhanced therapeutic approaches to address this formidable variant of liver cancer. The complex molecular landscape of HCC, characterized by aberrant signaling and genetic heterogeneity, underscores demand for innovative therapeutic approaches (Foerster et al., 2022; Su et al., 2022).

Angiogenesis, the complex process of vascular development, is elementary to growth and metastasis of neoplastic cells in hepatocellular carcinoma (HCC). This mechanism involves sprouting new branches from existing blood vessels or production of endothelium to establish

new capillaries, providing necessary nutrients and O₂ to neoplastic cells and promoting tumor progression (Yang et al., 2021). The stability between pro- and anti-angiogenic factors impacts the behavior of HCC, underscoring its significance as prospective drug target. Among the pivotal angiogenesis regulators, vascular endothelial growth factor (VEGF) and associated receptor (VEGFR) stand out as promising targets for anti-cancer therapy. VEGF, a glycoprotein in extracellular area, aids in establishing new vasculature within tumors, stimulating endothelial cell sprouting, mitogenesis, and migration (Choucair et al., 2021). It is critical for vasculogenesis during embryonic growth and vessel repair. VEGF binds to specific receptors, including VEGFR1 (works together with VEGF-A & B, and is a placenta growth factor) and VEGFR2 (the primary signaling receptor for VEGF-A). Additionally, VEGFR3 involved in lymphangiogenesis and can bind VEGF-C and VEGF-D following proteolytic cleavage. Given the VEGF implication in cancer angiogenesis, researching VEGF and its associated receptors has emerged as a promising approach for anti-cancer therapy. VEGF signaling inhibition can effectively suppress cancer proliferation and metastasis through

^{*} Corresponding author at: Department of Zoology, College of Science, King Saud University, P. O. Box 2455, Riyadh 11451, Saudi Arabia.
E-mail address: 444204108@student.ksu.edu.sa (H. Almasoud).

<https://doi.org/10.1016/j.jksus.2024.103407>

Received 2 June 2024; Received in revised form 14 August 2024; Accepted 21 August 2024

Available online 30 August 2024

1018-3647/© 2024 The Author(s). Published by Elsevier B.V. on behalf of King Saud University. This is an open access article under the CC BY license (<http://creativecommons.org/licenses/by/4.0/>).

intervening with newer blood vessels formation (Yang et al., 2021). Ramucirumab, an antagonist of VEGFR-2, has illustrated potential anti-angiogenic activity in many cancers, including HCC. Its efficacy stems from its competence to impede VEGF pathway, hence inhibiting angiogenesis of cancer and impairing tumor growth. However, regardless of its promising treatment prospects, monotherapy with Ramucirumab might be limited because of emerging issues of resistance mechanisms and incomplete tumor responses (Choucair et al., 2021). Epigenetic variations, for instance DNA methylation, represent another hallmark of cancer, contributing to growth and therapeutic resistance of tumor. 5-Aza-cytidine (5-Aza), a DNA methyltransferase inhibitor, has shown significance to reverse aberrant DNA methylation patterns and restore the tumor suppressor genes expression found within HCC patients. At low doses, 5-Aza demonstrates its efficacy by activating silenced tumor suppressor genes through demethylation of their promoter regions (Oosterom et al., 2018, Wang et al., 2019). This reactivation of genes holds an ability to restore their normal functionality, thereby aiding in cancer growth regulation. Conversely, higher doses of 5-Aza exhibit toxicity in carcinoma, further contributing to its therapeutic efficacy. The dual action, encompassing both gene reactivation and cytotoxicity, positions 5-Aza-cytidine as potential therapeutics for cancer management (Klose and Bird, 2006; Garcia-Manero et al., 2022; Kim et al., 2023). Combination treatment is gaining traction as a rational approach to enhance its treatment effectiveness and overcome resistance mechanisms in cancer. However, the optimal combination partners and their synergistic effects still to be unearthed, particularly in HCC. Combination therapy involving Ramucirumab with 5-Aza-cytidine, holds potential of targeting both the vascular microenvironment and epigenetic modifications inside cancer cells. This rational combination strategy holds significance to enhance treatment efficacy, overcome resistance mechanisms, and improve clinical outcomes in HCC patients. In this work, we assessed the potential synergistic therapeutic effects of combining Ramucirumab with 5-Aza-cytidine for HCC using the Human Hepatoma (HuH-7) cell line as a model system. Through a comprehensive measurement of cell viability, apoptosis, angiogenesis, and genetic profiling, we elucidated mechanistic of both drugs for HCC therapy.

2. Materials and methods

2.1. Preparation of drugs

The stock solution of 5-Aza was prepared in (DMSO) at a concentration of 100 mg/ml and further diluted to yield the tested concentration (1 μ M). 5-Aza was applied three days pre-treatment. Based on the detected IC₅₀, three doses (50, 100, and 150 μ g/ml) of Ramucirumab were investigated alone and in combination with 5-Aza.

2.2. Cell culture

HuH-7 cells were cultured in 10 % supplemented medium Dulbecco, modification of eagles DMEM with Fetal Bovine Serum FBS in addition to 1 % Penicillin at 37 °C in Humidified atmosphere containing 5 % CO₂ (Mishra et al., 2023). Based on experiments, cells were cultured in 96, 24 well plate, or 25-T flasks. The growing cells were washed with PBS and treated with trypsin. The collected cells were spun down at 1600 rpm for five min at 4 °C, then cells were diluted with medium at density 5x10⁵ cells/ml.

2.3. Cell viability assessment

Evaluation of cell viability was completed via earlier reported methods (Machado et al., 2019). Cells were initially seeded at density of 5 x 10⁵ cells/ml and allowed for incubation for 24 h. Subsequently, they were subjected to diverse concentrations of Ramucirumab; 20, 40, 80, 120, 150, and 220 μ g/ml and incubated for 24 hrs. Then, MTT assay reagent was put and left for incubation for 2 hrs at 37 °C, and then

agitation for 15 mins. Before measuring absorbance at 570 nm by spectrophotometer (Synergy-H1; BioTek).

2.4. Evaluation of intracellular ROS generation

We assessed ROS generation using the ROS assay kit (Sigma-Aldrich St. Louis, MO, USA). The cells were seeded in both 96-well black microplates and 6 microwell plate at 5x10⁵ cells/ml in 10 % cultured media and incubated for 24 h (37 °C). Subsequently, cells underwent the described treatment and incubation for another 24 h. Following treatment, the culture media was eliminated, while fresh media (100 μ l) was agitated with 5X concentration of H₂DCF dye solution/well in 96-well plate, while same solution (1 ml) was added per well in the 6-well plate. Later, incubation for one hour (37 °C) was performed. Measurement of absorbance within range of 485–528 nm. For visualization purposes, after removing the media from the 6 well-plates, thorough rinsing with 1xPBS was performed, and fluorescence microscope (DMLB, Leica, Germany) was utilized to capture images (Alkahtane et al., 2018).

2.5. Assessment of superoxide dismutase (SOD) and catalase (CAT) activities

Cells were initially seeded in 25 ml flask at 1x10⁶/ml (density) and kept for incubation for about 24 hrs. After incubation, cells were given diverse concentrations of Ramucirumab (50, 100, and 150 μ g/ml alone or in combination with 5-Aza) for further 24 h (temp. 37 °C). Cells were then gathered and rinsed with 1xPBS. Subsequently, cell lysis was lysed and collected using a cold buffer solution, followed by sonication for 5 mins with 1 mL of a buffer containing mannitol (210 mM), EGTA (1 mM), HEPES (20 mM), and dH₂O 100 ml at pH 7.2. After that, centrifugation of lysed cell suspension at 1500 rpm and (temp. 4 °C) for 5 minutes to gather supernatant was performed. Cayman SOD kit No.706002 was utilized to evaluate SOD activity. In a 96-microwell plate, diluted radical detector (200 μ L) was merged with 10 μ L of sample/well. The reaction was started through pouring of 20 μ L of diluted Xanthine Oxidase to every well, accompanied through 30-minute incubation and shaking (Alhoshani et al., 2022). Absorbance was measured within 440–460 nm range. For CAT, cells were seeded with drugs as mentioned earlier. Subsequently, further incubation of cells was performed for 24 h (temp. 37 °C). Post-incubation, 1X PBS was utilized to wash the cells and then catalase assay buffer was introduced for sonication for about five minutes. Then, centrifugation at 10,000 rpm of these sonicated cells at 4 °C for 10 mint, and collection of supernatants was done out. Catalase assay (BioVision, Catalog No. K773-100) was conducted by pouring 2 μ L of sample to assay buffer up to 78 μ L in every well of 96-well plate, followed by incubation at 25 °C for 5 min. Subsequently, developer mix of 50 μ L (catalase assay buffer (46 μ L), OxiRed TM Probe (2 μ L), HRP lyophilized solution (2 μ L)) was poured in every well, and incubated at 25 °C for 10 mint (Al-Zharani, 2024). Finally, measurement of absorbance was performed at 570 nm.

2.6. Evaluation of glutathione (GSH) levels

Cells initially seeded in 25 ml flask at density (1 x 10⁶/ml) were incubated for 24 hrs (temp. 37 °C). Subsequently, cells were exposed to the aforementioned treatments and allowed for another incubation for 24 h (temp. 37 °C). Following experimentation, cells were then rinsed in 1x PBS and subsequently cell lysis and gathered was performed with 1 ml of cold buffer solution, followed by sonicating for about 5 min. Then centrifugation of sonicated cell suspension at 1500 rpm for mins (temp. 4 °C), and final supernatant was delicately passed to another fresh 1.5 mL tube. The evaluation of GSH levels was performed using the Cayman GSH kit No.703002 according to producer's guidance. Briefly, 50 μ L sample was combined with 150 μ L of a cocktail containing MES Buffer, reconstituted cofactor, reconstituted enzyme, deionized H₂O,

and 5,5'-dithio-bis-2-nitrobenzoic acid. Then, incubation of plate in dark room for 25 min in, and measurement of absorbance at 410 nm was conducted (Alhoshani et al., 2022).

2.7. Hoescht assay for assessment of cell viability

The Hoechst dye assay stands as a widely employed staining method within cell biology and fluorescence microscopy. It harnesses fluorescent dyes belonging to the Hoechst family, such as Hoechst 33,342 or Hoechst 33258. These dyes, known for their DNA-binding properties, selectively label cellular nuclei, facilitating precise visualization under a microscope. HuH-7 cells were placed onto a 6-well plate with a cover slip placed at the centre, at 2×10^4 cells per well (density) (volume: 2 ml media per well), and incubated for 24 hrs at temp 37°C . Cells were subjected to three concentrations of Ramucirumab alone, 5-Aza alone, and combined therapy of three concentrations of Ramucirumab and 5-Aza for 24 hrs. Following period of incubation, media was detached, and cells were cleaned twice with 1X dilution buffer (10X: 5 ml of buffer (diluted) was poured to 45 ml dH₂O). Fixation was done with 3 % formaldehyde solution (sufficient to cover the dish) for 10–20 min. After removal of the fix solution, cold methanol (-20°C) was poured for about 20 min (Permeabilization step) at room temp. Following permeabilization, cells were rinsed (3–5 times) with phosphate buffer saline. Subsequently, Hoechst Dye solution (300 μL) containing 0.5 μL of Hoechst dye dissolved in 10 ml PBS was poured in all wells, and incubated at temp 37°C in an unilluminated environment for 10–20 min. Subsequent period of incubation, cells were rinsed (3–5 times) again with PBS, and the cover slips were relocated to microscopic slides.

2.8. Mitochondrial membrane potential (MMP) assay

HuH-7 were set on centre of cover slips in six-well plate at 2×10^4 cells/well (density) (volume: 2 ml media per well) and left to incubate for about 24 hrs at (temp. 37°C). Afterwards, treatment of cells at three concentrations of Ramucirumab alone, 5-Aza alone, and combined therapy of three concentrations of Ramucirumab and 5-Aza for 24 h. Following this, the media was detached, and cleaned through 1X dilution buffer (10X: 5 ml of dilution buffer was poured to 45 ml dH₂O). Subsequently, 1 ml of working JC-1 solution (JC-1 (500 μg) dissolved in DMSO (766.8 μL) was poured to all wells, and incubation of cells in an unilluminated environment for 10–20 min (37°C). After incubation, washing of cells (three-five times) with phosphate buffer saline, and then cover slips were transferred to microscope slides. Confocal microscope (CRCL's LSM 780 NLO confocal microscope) was used to capture images. In parallel experiment, ratio of JC-1 aggregates to monomers was determined as follows: seeding of HuH-7 cells in ninety six-well dark plate at 5×10^4 cells/well (density) for a day at (temp. 37°C). Next, cells were treated with three concentrations of Ramucirumab alone, 5-Aza alone, and Ramucirumab and 5-Aza for 24 h. Following incubation, the media were taken off, and cells were rinsed with 1X dilution buffer (10X: 5 ml of dilution buffer was introduced to 45 ml dH₂O). Subsequently, 1 ml of working JC-1 solution (500 μg of JC-1 dissolved in 766.8 μL of DMSO) was added in every well, and incubated in dark for 10–20 min at 37°C . Absorbance was estimated at wavelengths (535–590 nm) (aggregate excitation only) or (485–528 nm) (for monomer excitation) with microplate reader-(Gen5™ BioTek Cytation 5™, USA).

2.9. Analysis of gene expression

RNA samples were initially purified and utilized for cDNA synthesis using a cDNA kit (ThermoFisher USA, Cat No.00881457). The resulting cDNA was subjected to PCR amplification, and the products were confirmed through agarose gel electrophoresis. RT-PCR was then conducted to ascertain target sequences of apoptotic-related genes (Bcl2, Bax, p53, Cas-3, Cas-7, and Cas-9) subsequent treatment with drugs for

24 h. Fluorescence detection was employed to visualize amplification products, and fold expression calculation was done through $2^{-\Delta\Delta\text{CT}}$ method. However, amplification products, with fold expression calculated through $2^{-\Delta\Delta\text{CT}}$ method (Shoichiro et al., 2004).

2.10. Statistical analyses

Data obtained were subjected to one-way analysis of variance (ANOVA) and significant p-values were described as follows: * $p < 0.05$, ** $p < 0.01$, *** $p < 0.001$.

3. Results

3.1. Ramucirumab reduced viability of HuH-7 cells

The MTT assay examined the influence of Ramucirumab on growth of HuH-7 cells. Cells were exposed with 20 to 220 $\mu\text{g}/\text{mL}$ of Ramucirumab for 24 hrs. As depicted in (Fig. 1), a dose-dependent decline in survival was clearly noticed for each concentration inducing significant depletion in viability of cells.

3.2. Combinational treatment reduced intracellular ROS generation in HuH-7 cells

This imbalance between oxidants and antioxidants favors growth of tumors and ROS generation is an emerging hallmark of neoplastic cells that could act as a biomarker of effective cancer treatment. We investigated intracellular ROS levels in HuH-7 cells with either Ramucirumab or 5-Aza alone or co-treatment. Results demonstrated that Ramucirumab prompted a dose-dependent rise in ROS while 5-Aza also significantly increased intracellular ROS (Fig. 2). Contrastingly, co-exposure of the HuH-7 cells to both 5-Aza and Ramucirumab reduced intracellular ROS. However, the levels in an intracellular ROS post-exposure to both 5-Aza and 50 $\mu\text{g}/\text{mL}$ of Ramucirumab were still remarkably greater than in unexposed control cells ($p < 0.01$). Furthermore, co-exposure with Ramucirumab. This finding suggests that combinational treatment of the HuH-7 cells suppresses ROS generation.

3.3. SOD and CAT activity is induced by co-exposure of HuH-7 cells to 5-Aza and Ramucirumab

The observation that both Ramucirumab and 5-Aza suppressed ROS generation led to the investigation of SOD activity in the cells. SOD converts superoxides such as hydroxyl and oxygen radicals to hydrogen peroxides which are subsequently metabolized by catalase into water and oxygen molecules. Our findings showed that Ramucirumab alone

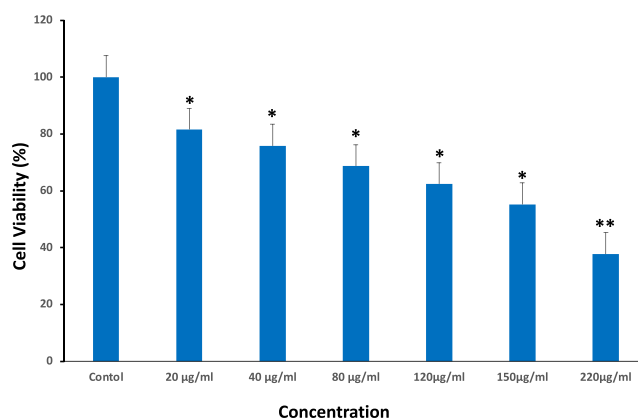


Fig. 1. Cell viability of HuH-7 cells after subjected to Ramucirumab for 24 hrs as assessed through MTT assay. Each value depicts the mean SE \pm ($n = 3$), (* $p < 0.05$, ** $p < 0.01$) compared to untreated group (control).

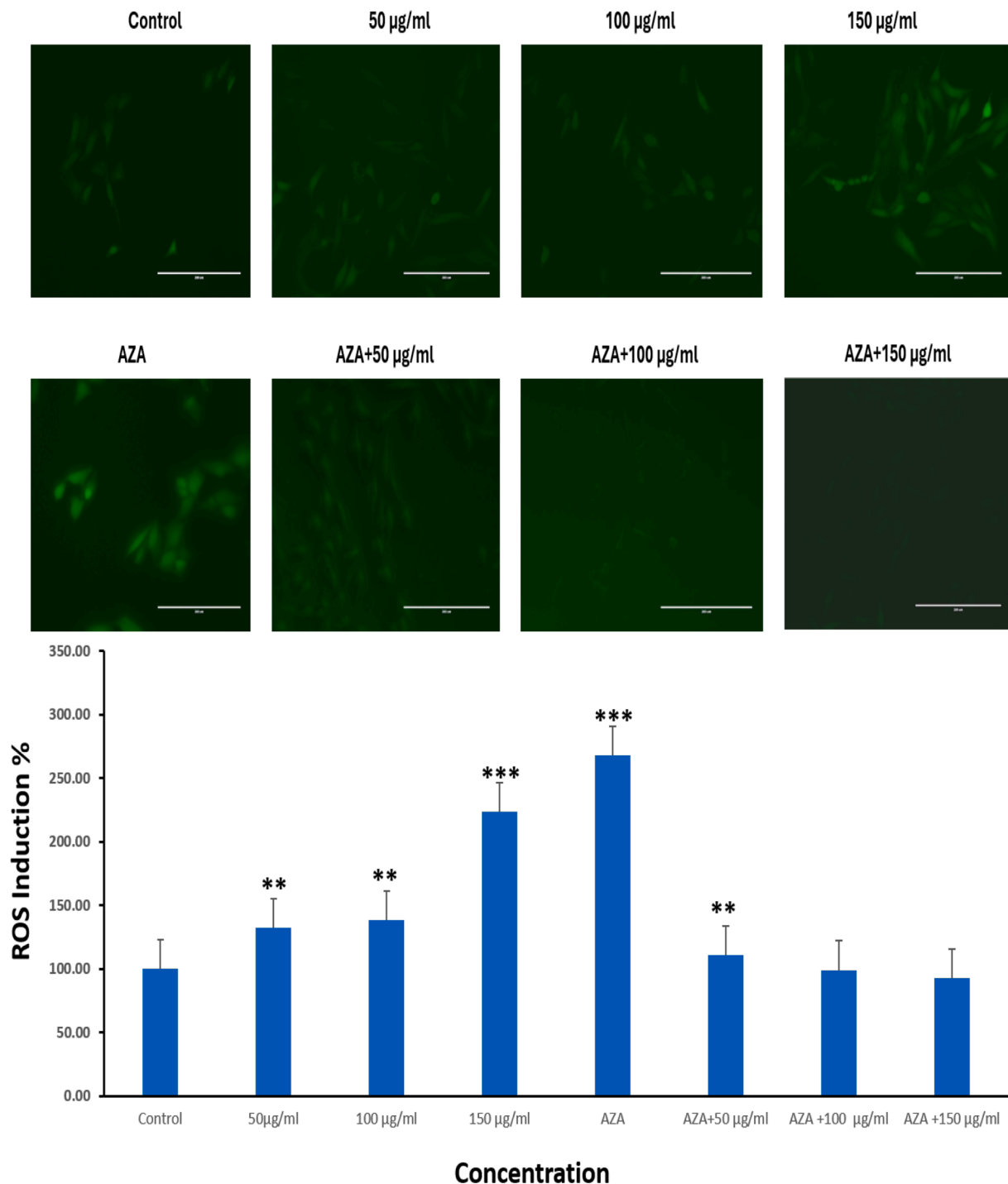


Fig. 2. ROS induction (%) in HuH-7 cells after subjected to Ramucirumab and 5-Aza for 24hr. Each value depicts the mean SE ± (n = 3), (**p < 0.01, ***p < 0.001) compared with control group.

caused significant suppression of SOD activity at both (100 and 150 µg/ml) concentrations (p 0.05) (Fig. 3A). In contrast, 5-Aza alone resulted in substantial elevation in SOD activity (p < 0.05). Similar to 5-Aza effect on SOD, the combinational treatment of HuH-7 cells by both Ramucirumab (all concentrations) and 5-Aza significantly increased SOD activity. This may indicate a response of SOD to increasing ROS levels in cells for ensuring redox balance.

As a confirmatory experiment, we investigated enzymatic activity of CAT in relation to the exposure conditions above. Findings showed that catalase activities increased in a dose-dependent way for Ramucirumab exposure for concentrations of 50 and 100 µg/ml. However, 150 µg/mL

Ramucirumab did not influence catalase activities. While 5-Aza exposure alone significantly prevented the activity of catalase (p < 0.05), a dose-dependent and considerable surge in activity was observed for co-exposure at all concentrations (Fig. 3B). These findings highlight the intricate interplay between these agents and cellular antioxidant pathways, providing insights into their potential synergistic effects in combating oxidation-induced stress in neoplastic cells.

3.4. Co-exposure of HuH-7 cells suppressed GSH levels

GSH is an intracellular ROS scavenger. When considered with ROS

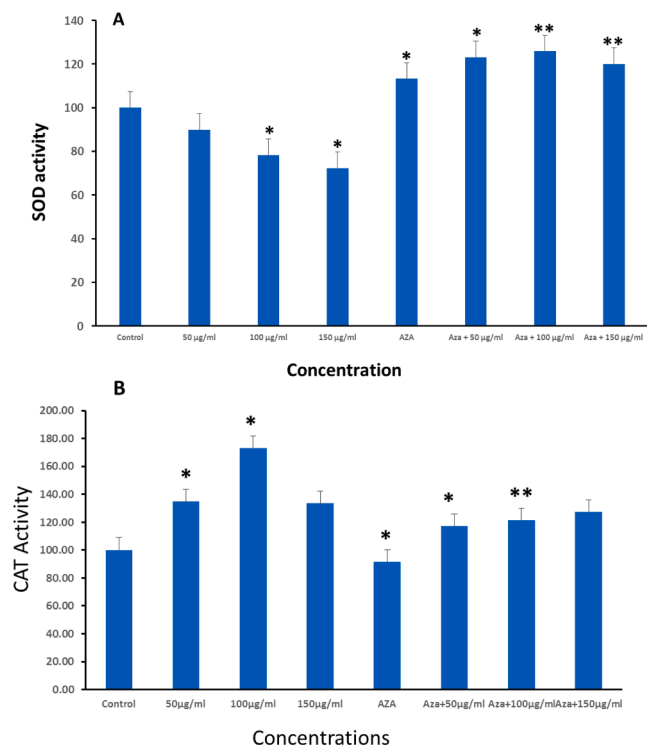


Fig. 3. HuH-7 cells were subjected to Ramucirumab, 5-Aza or a combined treatment with both drugs for 24hr. The cells were then evaluated for (A) SOD activity. (B) CAT activity. Data is shown as mean ± SE of n = 3 experiments. (**p* < 0.05 ***p* < 0.01) compared to untreated group (control).

levels, GSH levels signals the redox balance in intracellularly. It was noticed that exposure to Ramucirumab only did not influence GSH levels, as illustrated in Fig. 4. However, 5-Aza exposure was responsible for notable elevation in GSH levels identical to the combination of 5-Aza and 50 µg/ml Ramucirumab (*p* < 0.05). In addition, co-exposure HuH-7 cells to 5-Aza and 100 µg/mL or 150 µg/mL Ramucirumab cause even significantly higher GSH levels (Fig. 4).

3.5. Combination of Ramucirumab and 5-Aza induced DNA fragmentation

Upon discovering that either or both Ramucirumab and 5-Aza induced some level of redox imbalance, as evidenced by altered GSH and ROS levels alongside changes in CAT and SOD activity, we proceeded to investigate the possibility of DNA damage using Hoechst dye staining. Redox imbalance, characterized through oxidation-induced

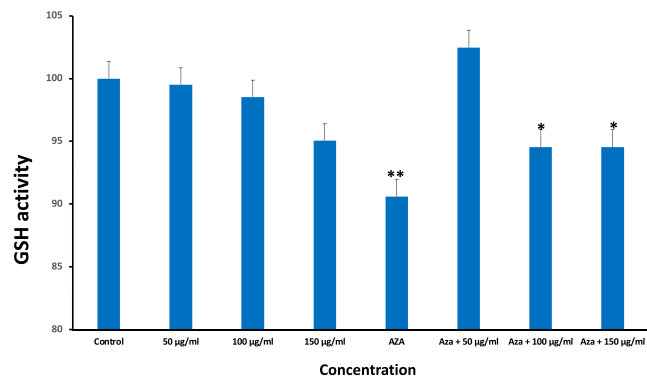


Fig. 4. GSH activity in HuH-7 cells after treatment with Ramucirumab and 5-Aza for 24hr. Each value represents the mean SE ± (n = 3), (**p* < 0.05 ***p* < 0.01) compared with control group.

stress, can cause significant cellular damage, including DNA fragmentation. As shown (Fig. 5), treatment with all concentrations of Ramucirumab or 5-Aza alone, and also 5-Aza combination with Ramucirumab at 50, 100, and 150 µg/ml, resulted in observable DNA damage in HuH-7 cells. The Hoechst dye that binds with minor groove of DNA highlighted these changes, indicating increased nuclear fragmentation and condensation of chromatin, which are hallmark features of DNA insult and apoptosis. This DNA damage reveals that combinational exposure of Ramucirumab and 5-Aza might have resulted in synergistic action, exacerbating cellular stress than otherwise expected from the action of single agent. This finding has significant implications, as it points to future prospect of combined therapy to improve efficacy of treatment against HuH-7 cells by not only inducing redox imbalance but also directly causing genetic damage, thereby promoting apoptosis.

3.6. Singular exposure of Ramucirumab or co-exposure to Ramucirumab and 5-Aza caused mitochondrial membrane damage

Assessment of MMP involves analyzing the changes in MMP and also

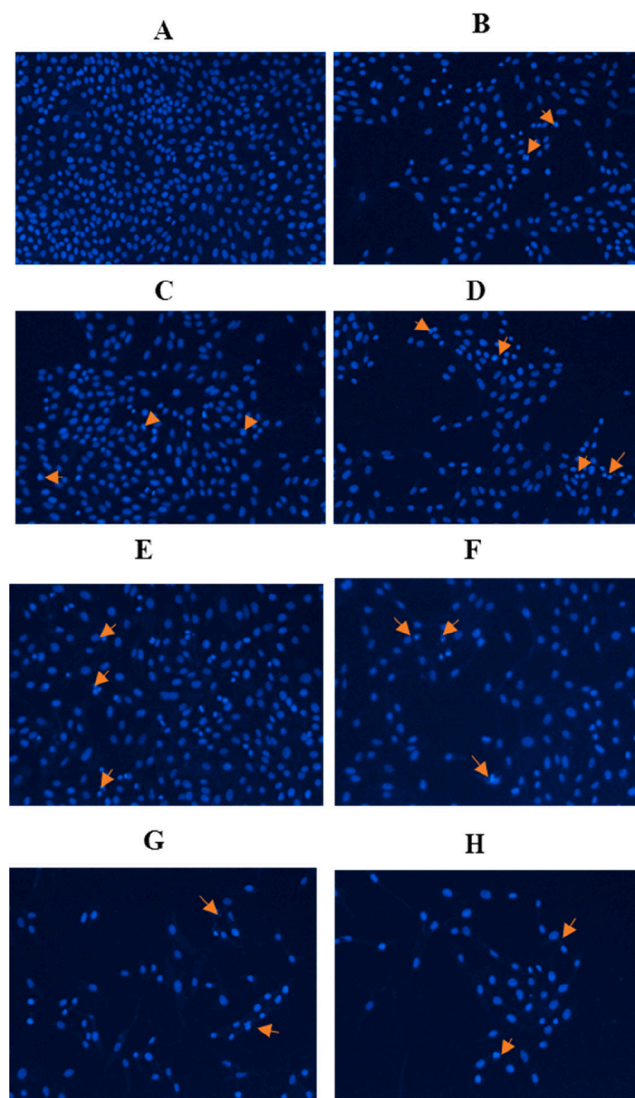


Fig. 5. Hoechst 33,342 staining, illustrating condensation of chromatin and fragmentation of DNA in Huh-7 cells subjected to various treatments (x20): (A) control, (B) Ramucirumab at 50 µg/mL, (C) Ramucirumab at 100 µg/mL, and (D) Ramucirumab at 150 µg/mL. (E) 5-Aza, (F) 5-Aza + Ramucirumab at 50 µg/mL, (G) 5-Aza + Ramucirumab at 100 µg/mL, (H) 5-Aza + Ramucirumab at 150 µg/mL.

apoptotic cell death in HuH-7 cells using two fluorescent dyes. These dyes stain healthy mitochondria (high MMP) with red fluorescence and damaged mitochondria (low MMP) with green fluorescence. The JC-1 aggregate/monomer ratio declined in Huh-7, in a dose-dependent manner. Fig. 6 A, B, and C illustrated loss of mitochondrial membrane potential in HuH-7 cells subjected to (A) three Ramucirumab concentration for 24 hrs (B) 1 μ M of Aza or combination of Aza and Ramucirumab for 24 hrs (C) Graphical illustration of MMP levels in HuH-7 cells after treating cells at various concentrations of Ramucirumab alone or co-treatment with 5-Aza for 24 hrs. Tests were conducted in triplicate (** $p < 0.05$, *** $p < 0.001$) and comparison was performed with control

group. Similarly, a singular dose of Aza at 1 μ M and the combinational exposure for all examined concentrations of Ramucirumab also demonstrated a dose-dependent depletion in JC-1 aggregate/monomer ratio. These are suggestive of MMP depletion, highlighting its role in inducing apoptosis in HuH-7 cells (Fig. 6).

3.7. Co-exposure to Ramucirumab and 5-Aza differentially influence apoptotic genes

Oxidative balance in neoplastic cells is a crucial aspect for maintaining cell viability or activating the cell-death pathways (Kuo et al.,

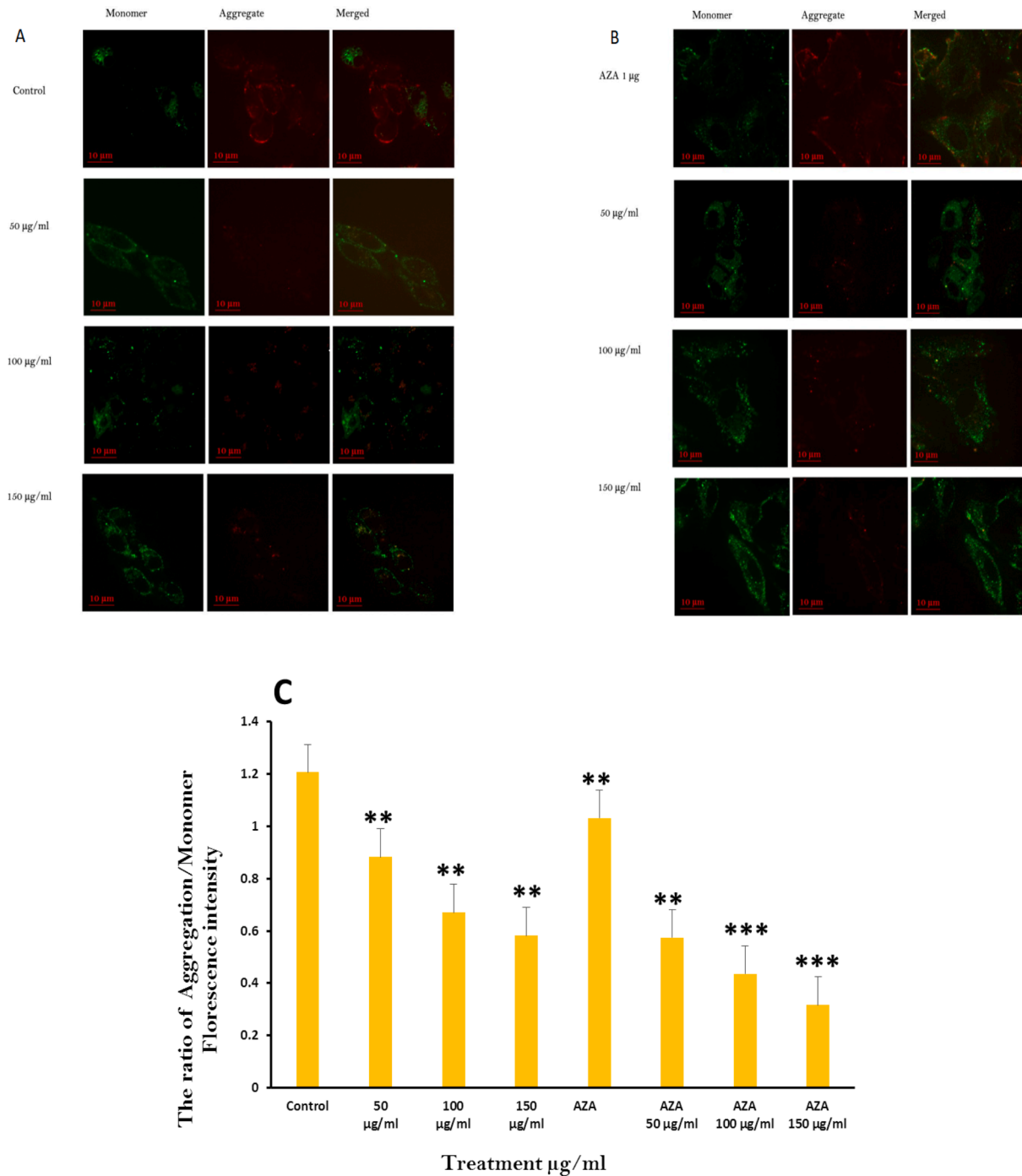


Fig. 6. Loss of mitochondrial membrane potential in HuH-7 cells subjected to (A) three Ramucirumab concentration for 24 hrs (B) 1 μ M of Aza or combination of Aza and Ramucirumab for 24 hrs (C) Graphical illustration of MMP levels in HuH-7 cells after treating cells at various concentrations of Ramucirumab alone or co-treatment with 5-Aza for 24 hrs. Tests were conducted in triplicate (** $p < 0.05$, *** $p < 0.001$) and comparison was performed with control group.

2022). We explored the gene expression of various apoptotic proteins including Caspases 3, 7, and 9. Moreover, p53, Bax, and Bcl-2. Upon exposure to Ramucirumab, our data supported that Ramucirumab induced a significant expression of cas-7 and -9 for every concentration while only 50 $\mu\text{g}/\text{mL}$ significantly increased cas-3 expression ($p < 0.05$) (Fig. 7). Similarly, 5-Aza significantly enhanced all the caspases expressions, similar to co-treatment with 5-Aza and Ramucirumab for each concentration ($p < 0.01$). This highlights that treatment of HuH-7 might be undergoing apoptotic cell death post-exposure to alone or combination of Ramucirumab and 5-Aza. Bax and Bcl2 are pro-apoptotic and anti-apoptotic proteins respectively acting upstream in the intrinsic apoptotic cell death pathway. Gene expression assessment of Bax showed that Ramucirumab and 5-Aza individually and in combinational exposure while only exposure to 5-Aza and 150 $\mu\text{g}/\text{mL}$ Ramucirumab enhanced gene expression of Bcl2. As for p53, exposure to 5-Aza either alone or with Ramucirumab enhanced the p53 expression in same manner as the exposure to all tested concentrations of Ramucirumab alone.

4. Discussion

Ramucirumab is a human IgG1 monoclonal antibody that exhibits a strong affinity for human VEGFR-2, effectively preventing the binding of VEGF-A, -C, and -D to their receptor. This interference with ligand-receptor interactions hinders VEGFR-2 activation and the subsequent signaling cascades essential for angiogenesis (Goel and Sun, 2015; Goel et al., 2016; Cheng et al., 2023). Ramucirumab has been approved as a single treatment option for HCC patients with α -fetoprotein levels ≥ 400 ng/mL who have also undergone prior treatment with sorafenib, an inhibitor of angiogenesis also targeting the VEGF pathway. In the present research study, we investigated combinational therapy involving Ramucirumab and 5-Azacytidine, which inhibits the methylation of DNA, thereby preventing neoplasticity of cancer cells. Evaluation of

Ramucirumab's impact on HuH-7 Cell Viability showed dose-dependent reduction in HuH-7 cell viability on exposure to Ramucirumab. This corroborates previous findings highlighting its anti-proliferative properties across cell lines of various carcinomas. For example, Refolo et al. (2020) demonstrated that 100 $\mu\text{g}/\text{mL}$ Ramucirumab significantly inhibited cell viability and proliferation of various gastric tumor cells such as KATOIII, HGC and N87 cell lines. Another research study by D'Alessandro et al. (2019) also demonstrated that 600 μM or Ramucirumab significantly inhibited cell survival of HepG2 cell lines. Literature reports also suggested that Ramucirumab complexed with other small molecule inhibitors (SMIs) significantly enhanced anticancer action of SMIs. Taha et al. (2022) showed that Ramucirumab enhanced sensitivity of different gastrointestinal tumor cell lines to the anticancer effect of sorafenib. D'Alessandro et al. (2019) also reported that Ramucirumab sensitizes gastrointestinal carcinoma to low dose of regorafenib and sorafenib. Taken together, results of the above investigations align with the suggestion of Ramucirumab efficacy as a monotherapy and/or as combined regimens in different cancers. However, the mechanism of action triggering cytotoxic mechanism of action triggering cytotoxic action on specific carcinoma cell lines warrant further investigation. Elevated amount of intracellular ROS often precedes intrinsic apoptotic pathway activation. The reduction in intracellular ROS levels observed upon co-exposure to Ramucirumab and 5-Aza may demonstrate potential synergistic effect in mitigating oxidative damage that often implicated in cancer progression. However, the differential effects of Ramucirumab and 5-Aza on SOD and catalase activities highlight elaborate interaction between these agents and cellular antioxidant pathways. While Ramucirumab suppressed SOD activity, potentially exacerbating oxidative stress, 5-Aza exhibited contrasting effects, indicating a nuanced regulation of antioxidant defense mechanisms. Low levels of GSH and high amounts of intracellular ROS are of relevance with reference to Ramucirumab exposure which may signal oxidative stress or redox imbalance. Interestingly, apoptosis has been implicated

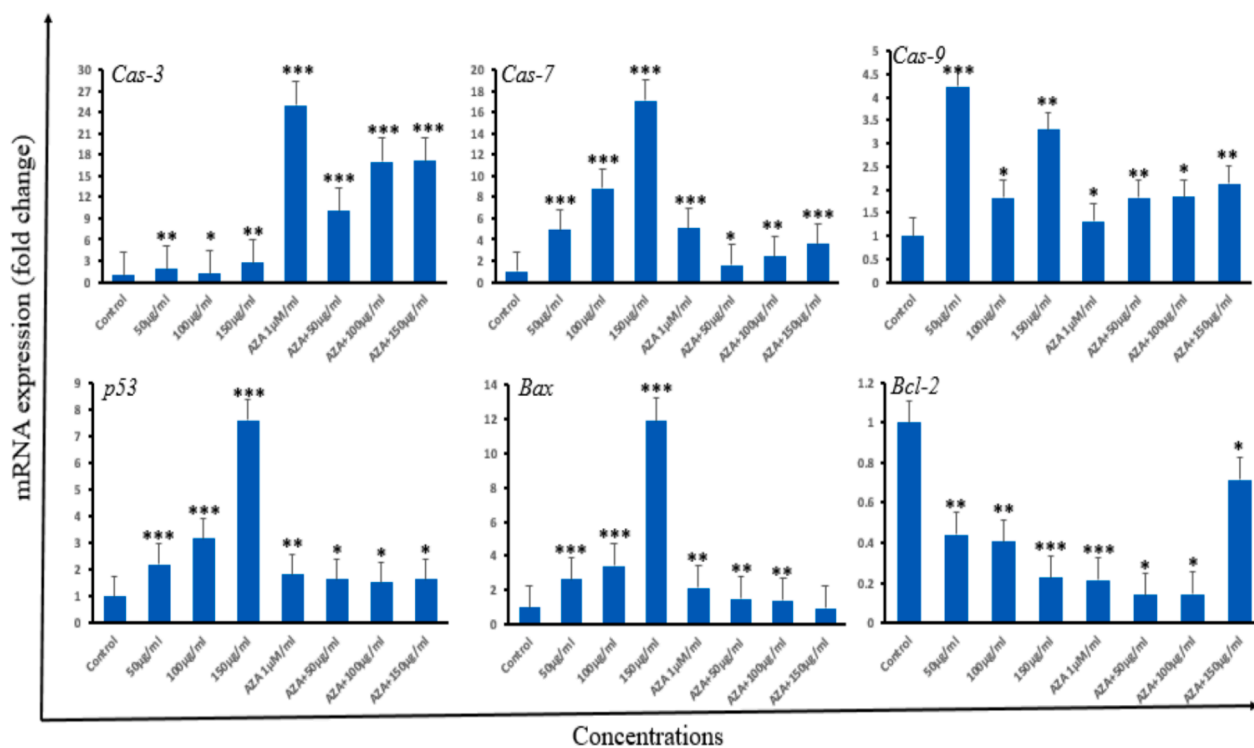


Fig. 7. Fold-change in apoptotic genes expression in HuH-7 cells as analyzed by real-time PCR (qPCR). HuH-7 cells were subjected to different doses of Ramucirumab or 5-Aza alone, and combined therapy with Ramucirumab and 5-Aza for 24 hrs. The genes measured were Cas-3, Cas-7, Cas-9, p53 Bax and Bcl-2. Data is shown as mean \pm SD of $n = 3$ experiments. Statistical significance is indicated as follows: * $p < 0.05$, ** $p < 0.01$, *** $p < 0.001$ and comparison was performed with control group.

to happen due to reduction in cellular GSH by itself. 5-Aza may reactivate silenced genes involved in antioxidant defense mechanisms, leading to apoptosis and/or increased SOD and CAT activity. The combination treatment may reduce ROS levels and enhance antioxidant enzyme activity, balancing cellular redox status. Moreover, combination may improve DNA repair mechanisms, and increased free radicals scavenging and oxidative damage. Furthermore, the active expulsion of cellular GSH has been hinted as a prospective trigger for apoptosis in diverse cell types. Similar results on redox imbalance have been discovered in various research studies. Yusuf and Casey (2020) showed that silver nanoparticles caused low intracellular ROS and high GSH levels in THP1 cell line inducing redox imbalance that led to apoptosis. Similarly, exposure of naïve PC12 cells to diamide resulted in redox imbalance with subsequent apoptosis activation. Pias and Yee Aw (2002) showed that introduction of PC12 cells led to no generation of ROS but an offset in the GSH/GSSG ratio which led to apoptosis was observed. The differential expression of apoptosis-related genes to drug exposure underscores the complex interplay between oxidative stress, apoptosis, and therapeutic interventions in cancer cells. The present work has delineated either or both of Ramucirumab and 5-Aza differentially modulated the caspases expression along with Bax and Bcl2. We interestingly found cells co-treated with both drugs to have high Bax/Bcl2 ratio, which could be plausibly justified by observed redox imbalance. Earlier research reports have proposed that redox imbalance in carcinomas favour activation of apoptotic genes especially higher levels in Bax to Bcl2 ratio. Bcl2 serves as protein for survival in neoplastic cells by halting interface of Bax and mitochondrial membrane, thus results preventing MOMP, release of cytochrome C through mitochondrion, and followed by caspase-dependent apoptosis activation (Li et al., 2016; Wang et al., 2019, Kuang et al., 2022). Current result of RT-PCR demonstrated upregulation of measured expression of caspases; 3, 7, 9, bax, and p⁵³. In contrast, Bcl-2 expression as an anti-apoptotic gene was significantly decreased after treatments. Caspases and bcl-2 work in opposite way. However, some studies reported that BCL-2 family interacting with other partners to either inhibit or induce cell death and this simultaneously action may explain the high expression of both tested caspases and bcl-2 (AL-johani et al., 2022). The elevation in Bax with concomitant reduction in Bcl2 expression in our study might have caused excessive protein binding of Bax with mitochondria causing MOMP and caspases 3 and 7 activation consequent upon the imbalance in redox factors within cell. Interestingly, our study showed decrease MMP which signals induction of MOMP. Similarly, we found high gene expressions of the executioner caspases 3, 7 and 9 in the current research work, in accord with earlier reports. As a tumor suppressor, p53 activity is central to regulating tumor development and advancement. Mutations in TP53 gene which encodes p53 protein for tumor suppression or its reduced expression is found in about 50 % of cancers. Mutations in the gene results in protein loss of function and this is linked to increase cancer cell survival. Here, we found significantly high TP53 gene expression with subsequent decrease in Bcl-2 gene expression. Previous research studies have found that under specific conditions, Bcl-2 transcription can be antagonized by p53. Moreover, the expression of p53 in p53 null cells led to depletion in Bcl-2 gene expression (Crowe and Sinha, 2006). Similarly, p53-induced expression via gamma irradiation also inhibited bcl-2 expression. For transcription-independent apoptosis, p53 might exert a direct effect on Bcl-2 activity through the binding of cytoplasmic p53 to Bcl-2 family. This interaction subsequently causes permeabilization of the mitochondria, thereby initiating apoptosis. The upregulation of caspases and other apoptotic genes, along with the decline in mitochondrial function, suggests that the observed phenotypic changes in cell viability and mitochondrial function are associated with the activation of apoptotic pathways. These findings indicate that the combination of Ramucirumab and 5-Aza may enhance apoptotic signaling, leading to reduced cell viability and mitochondrial dysfunction in HuH-7 cells. In addition, significant cytotoxicity in cancer cells, leading to cell death through the Pyroptosis pathway, which is

established by monitoring numerous associated with numerous events starting from organelles membranes damage to cell membrane demolition. Thus drugs design strategies are believed to have great potential in cancer therapy and the development of future drug candidates to mitigate cancers (Mishra et al., 2024).

5. Conclusion

Our findings offer insights into potential synergistic effects of Ramucirumab and 5-Aza. Ramucirumab, particularly when co-administered with 5-Aza, effectively reduces viability of cells and prompts apoptosis in HuH-7 cells through increased oxidative stress, disturbance of MMP, and apoptotic pathways activation. The combination treatment shows potential for enhanced therapeutic efficacy against hepatocellular cancer cells.

6. Availability of data and materials

The data generated or analyzed in this article are online publicly available without request.

7. Authors' contributions

Hadeel Almasoud, performed the cytotoxic assays, apoptotic gene expression, Mitochondrial Membrane Potential (MMP) Assay, and cells survival. Saud Alarifi, assessed the generation of iROS. Saad Alkahtani evaluated DNA damage. Saud Alarifi and Saad Alkahtani wrote and edited the article. All authors have approved the final article.

CRediT authorship contribution statement

Hadeel Almasoud: Validation, Software, Methodology, Investigation, Formal analysis, Data curation. **Saud Alarifi:** Writing – original draft, Methodology. **Saad Alkahtani:** Writing – review & editing, Supervision, Investigation, Funding acquisition, Conceptualization.

Declaration of Competing Interest

The authors declare that they have no known competing financial interests or personal relationships that could have appeared to influence the work reported in this paper.

Acknowledgement

This work was funded by Researchers Supporting Project number (RSP2024R26), King Saud University, Riyadh, Saudi Arabia.

References

- Alhoshani, N.M., Al-Johani, N.S., Alkeraishan, N., Alarifi, S.u., Alkahtani, S.a., 2022. Effect of lycopene as an adjuvant therapy with 5-flourouracil in human colon cancer. *Saudi J. Biol. Sci.* 29 (2022), 103392.
- AL-Johani, Norah, Mohammed Al-Zharani, Bader Almutairi, Nada H. Aljarba, Norah M. Alhoshani, Nora Alkeraishan, Saud Alarifi, Daoud Ali, Saad Alkahtani. (2022). Protective effect of coenzyme-10 and piperine against cyclophosphamide-induced cytotoxicity in human cancer HuH-7 cells. *Journal of King Saud University – Science* 34 (2022) 102009.
- Alkahtane, A.A., Alarifi, S., Al-Qahtani, A.A., Ali, D., Alomar, S.Y., Aleissia, M.S., Alkahtani, S., 2018. Cytotoxicity and genotoxicity of cypermethrin in hepatocarcinoma cells: a dose-and time-dependent study. *Dose-Response* 16 (2), 1559325818760880.
- Cheng, W.-C., Shen, Y.-C., Chen, C.-L., Liao, W.-C., Chen, C.-H., Chen, H.-J., Chih-Yen, Tu., Hsia, T.-C., 2023. Bevacizumab versus Ramucirumab in EGFR-mutated metastatic non-small-cell lung cancer patients: a real-world observational study. *Cancers* 15, 642. <https://doi.org/10.3390/cancers15030642>.
- Choucair, K., Kamran, S., Saeed, A., 2021. Clinical evaluation of ramucirumab for the treatment of hepatocellular carcinoma (HCC): place in therapy. *OncoTargets and Therapy* 5521–5532.
- Crowe, D.L., Sinha, U.K., 2006. p53 apoptotic response to DNA damage dependent on bcl2 but not bax in head and neck squamous cell carcinoma lines. *Head Neck* 28, 15–23. <https://doi.org/10.1002/hed.20319>.

- D'Alessandro, R., Refolo, M.G., Iacovazzi, P.A., Pesole, P.L., Messa, C., Carr, B.I., 2019. Ramucirumab and GSK1838705A enhance the inhibitory effects of low concentration sorafenib and regorafenib combination on HCC cell growth and motility. *Cancers* 11, 787. <https://doi.org/10.3390/cancers11060787>.
- Foerster, F., Gairing, S.J., Müller, L., Galle, P.R., 2022. NAFLD-driven HCC: safety and efficacy of current and emerging treatment options. *Journal of Hepatology* 76 (2), 446–457.
- Garcia-Manero, G., Döhner, H., Wei, A.H., La Torre, I., Skikne, B., Beach, C.L., Santini, V., 2022. Oral azacitidine (CC-486) for the treatment of myeloid malignancies. *Clin. Lymphoma Myeloma and Leukemia* 22 (4), 236–250.
- Goel, G., Sun, W., 2015. Ramucirumab, another anti-angiogenic agent for metastatic colorectal cancer in second-line setting-its impact on clinical practice. *J. Hematol. Oncol.* 8, 1–3.
- Goel, G., Chauhan, A., Hosein, P.J., 2016. Ramucirumab: a novel anti-angiogenic agent in the treatment of metastatic colorectal cancer. *Current Colorectal Cancer Reports* 12, 232–240.
- Kim, D.Y., Lee, R., Cheong, H.T., Ra, C.S., Rhee, K.J., Park, J., Jung, B.D., 2023. 5-Azacytidine (5-aza) induces p53-associated cell death through inhibition of DNA methyltransferase activity in Hep3B and HT-29 cells. *Anticancer Res.* 43 (2), 639–644.
- Klose, R.J., Bird, A.P., 2006. Genomic DNA methylation: the mark and its mediators. *Trends Biochem. Sci.* 31 (2), 89–97.
- Kuang, C., Park, Y., Augustin, R., Lin, Y., Hartman, D.J., Seigh, L., Pai, R.K., Sun, W., Bahary, N., Ohr, J., Rhee, J.C., Marks, S.M., Beasley, H.S., Shuai, Y., Herman, J.G., Zarour, H.M., Chu, E., Lee, J.J., Krishnamurthy, A., 2022. Pembrolizumab plus azacitidine in patients with chemotherapy refractory metastatic colorectal cancer: a single-arm phase 2 trial and correlative biomarker analysis. *Clin. Epigenetics* 14, 3.
- Kuo, C.-L., Ponneri Babuharisankar, A., Lin, Y.-C., Lien, H.-W., Lo, Y.K., Chou, H.-Y., Tangeda, V., Cheng, L.-C., Cheng, A.N., Lee, A.-Y.-L., 2022. Mitochondrial oxidative stress in the tumor microenvironment and cancer immunoescape: foe or friend? *J. Biomed. Sci.* 29, 74. <https://doi.org/10.1186/s12929-022-00859-2>.
- Li, W., Wu, D., Niu, Z., Jiang, D., Ma, H., He, H., Zuo, X., Xie, X., He, Y., 2016. 5-Azacytidine suppresses EC9706 cell proliferation and metastasis by upregulating the expression of SOX17 and CDH1. *Int. J. Mol. Med.* 38, 1047–1054.
- Machado, A.R.T., Aissa, A.F., Ribeiro, D.L., Costa, T.R., Ferreira Jr, R.S., Sampaio, S.V., Antunes, L.M.G., 2019. Cytotoxic, genotoxic, and oxidative stress-inducing effect of an l-amino acid oxidase isolated from *Bothrops jararacussu* venom in a co-culture model of HepG2 and HUVEC cells. *Int. J. Bio. Macromolecules* 127, 425–432.
- Mishra, S., Das, K., Chatterjee, S., Sahoo, P., Kundu, S., Pal, M., Bhaumik, A., Ghosh, C.K., 2023. Facile and green synthesis of novel fluorescent carbon quantum dots and their silver heterostructure: An in vitro anticancer activity and imaging on colorectal carcinoma. *ACS Omega* 8 (5), 4566–4577. <https://doi.org/10.1021/acsomega.2c04964>.
- Mishra, S., Sannigrahi, A., Ruidas, S., Chatterjee, S., Roy, K., Misra, D., Maity, B.K., Paul, R., Ghosh, C.K., Saha, K.D., Bhaumik, A., Chattopadhyay, K., 2024. Conformational switch of a peptide provides a novel strategy to design peptide loaded porous organic polymer for pyroptosis pathway mediated cancer therapy. *Small* 24, e2402953.
- Oosterom, N., Griffioen, P.H., Den Hoed, M.A.H., Pieters, R., Dejo Jonge, R., Tissing, W.J.E., Vanden Heuvel-Eibrink, M.M., Heil, S.G., 2018. Global methylation in relation to methotrexate-induced oral mucositis in children with acute lymphoblastic leukemia. *PLOS ONE* 13, e0199574.
- Pias, E.K., Yee Aw, T., 2002. Apoptosis in mitotic competent undifferentiated cells is induced by cellular redox imbalance independent of reactive oxygen species production. *FASEB J.* 16, 781–790. <https://doi.org/10.1096/fj.01-0784com>.
- Refolo, M.G., Lotesoriere, C., Lolli, I.R., Messa, C., D'Alessandro, R., 2020. Molecular mechanisms of synergistic action of Ramucirumab and Paclitaxel in Gastric Cancers cell lines. *Sci. Rep.* 10, 7162. <https://doi.org/10.1038/s41598-020-64195-x>.
- Shoichiro, O., Kagawa, S., Tango, Y., Umeoka, T., Tokunaga, N., Tsunemitsu, Y., Roth, J. A., Taya, Y., Tanaka, N., Fujiwara, T., 2004. Quantitative analysis of p53-targeted gene expression and visualization of p53 transcriptional activity following intratumoral administration of adenoviral p53 in vivo. *Mol. Cancer Therapeutics* 3, 93–100.
- Su, T.H., Hsu, S.J., Kao, J.H., 2022. Paradigm shift in the treatment options of hepatocellular carcinoma. *Liver Int.* 42 (9), 2067–2079.
- Sung, H., Ferlay, J., Siegel, R.L., Laversanne, M., Soerjomataram, I., Jemal, A., Bray, F., 2021. Global cancer statistics 2020: GLOBOCAN estimates of incidence and mortality worldwide for 36 cancers in 185 countries. *A Cancer Journal for Clinicians*, CA, pp. 1–41.
- Taha, A.M., Aboulwafa, M.M., Zedan, H., Helmy, O.M., 2022. Ramucirumab combination with sorafenib enhances the inhibitory effect of sorafenib on HepG2 cancer cells. *Sci. Rep.* 12, 17889. <https://doi.org/10.1038/s41598-022-21582-w>.
- Wang, S.C., Wu, C.T., Wu, D.Y., Chen, C.G., Chang, K.M., Chang, C.C., 2019. The impact of the epigenetic cancer drug azacitidine on host immunity: the role of myelosuppression, iron overload and tp53 mutations in a Zebrafish model. *Cancers (Basel)* 11.
- Yang, Y., Ren, L., Yang, H., Ge, B., Li, W., Wang, Y., Wang, J., 2021. Research progress on anti-angiogenesis drugs in hepatocellular carcinoma. *Cancer plus* 3 (2), 33.
- Yusuf, A., Casey, A., 2020. Liposomal encapsulation of silver nanoparticles (AgNP) improved nanoparticle uptake and induced redox imbalance to activate caspase-dependent apoptosis. *Apoptosis* 25, 120–134. <https://doi.org/10.1007/s10495-019-01584-2>.